Short-time critical dynamics of the three-dimensional Ising model

# Short-time critical dynamics of the three-dimensional Ising model

A Jaster†, J Mainville†, L Schülke† and B Zheng‡

† Universität GH Siegen, D-57068 Siegen, Germany
‡ Universität Halle, D-06099 Halle, Germany

**Abstract.** Comprehensive Monte Carlo simulations of the short-time dynamic behaviour are reported for the three-dimensional Ising model at criticality. Besides the exponent $\theta$ of the critical initial increase and the dynamic exponent $z$, the static critical exponents $\nu$ and $\beta$ as well as the critical temperature are determined from the power-law scaling behaviour of observables at the beginning of the time evolution. States of very high temperature as well as of zero temperature are used as initial states for the simulations.

## 1. Introduction

Critical properties of many magnetic materials can be described by a simple Ising model,

$$H = K \sum_{\langle i,j \rangle} S_i S_j \tag{1}$$

where $S_i = \pm 1$ represents the spin of site $i$, and the sum extends over nearest neigbours only. The factor $1/k_B T$ is included in the coupling constant $K$. The Ising model has been solved exactly in one and two dimensions. However, for higher dimensions, there exist extensive perturbative analyses based on renormalization group methods and numerical investigations with Monte Carlo methods.

It was traditionally believed that universal scaling behaviour exists only in or near thermodynamic equilibrium. Recently, it has been argued theoretically [1] that some dynamic systems already exhibit universal scaling behaviour in the macroscopic short-time region of their dynamic evolution. The main point is that universality and scaling emerge after a microscopic timescale $t_{\mathrm{mic}}$, which is sufficiently large in the microscopic sense but still short in the macroscopic sense. This statement has been proven valid in a series of numerical simulations of various statistical systems. More interestingly, as well as the new critical exponent $\theta$, describing the critical initial increase of the magnetization, and the dynamic critical exponent $z$, short-time critical dynamics provides a measure of the static critical exponents and of the critical temperature. This dynamic approach is free of critical slowing down since the spatial correlation length is still small within the short-time regime, even at or near the critical point§.

Up to now, systematic numerical simulations of the short-time critical dynamics have been carried out mainly in two-dimensional systems [2]. For the three-dimensional Ising model, the power-law decay of the magnetization starting from an ordered state has been simulated [3,4],

§ For a recent review see [2].

the new exponent $\theta$ and the dynamic exponent $z$ have also been obtained [5–7]. However, a complete understanding of the short-time dynamic behaviour of the three-dimensional Ising model is still necessary, since it is a very important model. Especially, a systematic test of the short-time dynamic approach to the determination of all the critical exponents and the critical temperature in a three-dimensional system is important.

In this paper we report a comprehensive investigation of the short-time critical dynamics of the three-dimensional Ising model. A power-law behaviour of the autocorrelation, the second moment and the Binder cumulant is observed, in addition to that of the magnetization. The results fully support the short-time dynamic scaling. For the first time we extract the critical temperature and the static exponents $\nu$ and $\beta$ from the short-time scaling behaviour. Our results for the static exponents and critical temperature agree well with those obtained in the extensive studies at thermodynamic equilibrium.

In the next section, a scaling analysis of the short-time critical dynamics is given. Numerical results are presented in section 3. The last section contains the summary and discussion.

## 2. Scaling relations

Using renormalization group methods, Janssen *et al* [1] have shown that far from equilibrium, in a macroscopic short-time regime of the dynamical evolution, there already emerges universal scaling behaviour in the $O(N)$ vector model. The relaxation process considered is one of a system initially in a high-temperature state, suddenly quenched to the critical temperature $T_c$ and evolving with dynamics of model A. For an initial state with a non-zero but small magnetization ($m_0 \ll 1$), a generalized dynamic scaling form has been derived with an $\epsilon$-expansion for the $O(N)$ vector model,

$$M^{(k)}(t, \tau, L, m_0) = b^{-k\beta/\nu} M^{(k)}(b^{-z}t, b^{1/\nu}\tau, b^{-1}L, b^{x_0}m_0). \tag{2}$$

In equation (2), $M^{(k)}$ is the $k$th moment of the magnetization,

$$M^{(k)}(t) = \frac{1}{L^3}\left\langle \left(\sum_i S_i(t)\right)^k \right\rangle \tag{3}$$

$t$ is the time of the dynamical relaxation, $L$ is the lattice size,

$$\tau = \frac{T - T_c}{T_c} \tag{4}$$

is the reduced temperature, and $b$ is a spatial rescaling factor. The quantity $x_0$ is a new independent critical exponent, the scaling dimension of the initial magnetization $m_0$. The interesting and important point is that the critical exponents $\beta$, $\nu$ and $z$ in equation (2) are exactly those usually defined in equilibrium. These exponents can thus be extracted from the short-time critical dynamics.

Equation (2) provides the time evolution of the magnetization, with $k = 1$. Taking $b = t^{1/z}$ for the spatial scaling factor gives

$$M(t, \tau, m_0) = t^{-\beta/\nu z} M(1, t^{1/\nu z}\tau, t^{x_0/z}m_0) \sim m_0\, t^{(x_0-\beta/\nu)/z} F(t^{1/\nu z}\tau) + \mathcal{O}([t^{x_0/z}m_0]^2). \tag{5}$$

The expansion has been performed with respect to the small quantity $t^{x_0/z}m_0$ and $M(t, m_0 = 0) = 0$ has been used. It has been implicitly assumed that $L$ is sufficiently large. Exactly at the critical point ($\tau = 0$), equation (5) predicts a power-law behaviour of the magnetization in the short-time region,

$$M(t) \sim t^\theta \qquad \theta = \left(x_0 - \frac{\beta}{\nu}\right)\frac{1}{z}. \tag{6}$$

Up to now, analytical calculations for the $O(N)$ vector model and numerical simulations for a variety of statistical systems show that $\theta > 0$, i.e. the magnetization undergoes an initial *increase*. This is a very prominent phenomenon in the short-time critical dynamics.

Now we consider the case $m_0 = 0$. Using equation (2) for the second moment of the magnetization at the critical temperature gives

$$M^{(2)}(t) \sim t^{-2\beta/\nu z} M^{(2)}(1, t^{-1/z}L). \tag{7}$$

In the beginning of the time evolution the spatial correlation length is still small, even at the critical point. Thus it can be deduced that $M^{(2)}(t, L) \sim L^{-d}$, where $d$ is the dimension of the system. Taking this into account, equation (7) yields a power-law behaviour

$$M^{(2)}(t) \sim t^{c_2} \qquad c_2 = \left(d - 2\frac{\beta}{\nu}\right)\frac{1}{z}. \tag{8}$$

An analysis of the autocorrelation (for $m_0 = 0$)

$$A(t) = \frac{1}{N}\left\langle \sum_i S_i(t)S_i(0)\right\rangle \tag{9}$$

shows that it obeys a power law [8]

$$A(t) \sim t^{-c_a} \qquad c_a = \frac{d}{z} - \theta. \tag{10}$$

In summary, simulations of the dynamic system starting from small or zero initial magnetization, at or near the critical point, allow the quantities $\theta$, $c_2$ and $c_a$ to be measured and thus a determination of the critical exponents $\theta$, $\beta/\nu$ and $z$ separately. In principle, the critical temperature itself can also be determined from the location of the optimal power-law behaviour of the magnetization within the critical region [2,9]. However, a similar but more accurate determination of the critical temperature will be presented below. This is also the case for the determination of the exponent $\nu$ from the derivative of $M$ with respect to $\tau$.

In the above considerations the dynamic relaxation process was assumed to start from a disordered state with vanishing or small magnetization $m_0$. Another interesting and important process is the dynamic relaxation from a completely ordered state. The initial magnetization being exactly at its fixed point $m_0 = 1$, a scaling form

$$M^{(k)}(t, \tau, L) = b^{-k\beta/\nu} M^{(k)}(b^{-z}t, b^{1/\nu}\tau, b^{-1}L) \tag{11}$$

is expected. This scaling form looks the same as the dynamic scaling form in the long-time regime, however, it is now assumed already valid in the macroscopic short-time regime.

For the magnetization itself, $b = t^{1/z}$ yields

$$M(t, \tau) = t^{-\beta/\nu z} M(1, t^{1/\nu z}\tau). \tag{12}$$

This leads to the power-law behaviour

$$M(t) \sim t^{-c_1} \qquad c_1 = \frac{\beta}{\nu z} \tag{13}$$

at the critical point ($\tau = 0$). For small but nonzero $\tau$, the power-law behaviour of the magnetization will be modified by the scaling function $M(1, t^{1/\nu z}\tau)$, thus allowing for a determination of the critical temperature [2]. Taking the derivative with respect to $\tau$ on both sides of equation (12) and fixing $b = t^{1/z}$ again, gives the logarithmic derivative of the magnetization

$$\partial_\tau \ln M(t, \tau)|_{\tau=0} \sim t^{-c_{\ell 1}} \qquad c_{\ell 1} = \frac{1}{\nu z}. \tag{14}$$

Here, unlike the relaxation from a disordered state, the average magnetization is not zero. A Binder cumulant $U(t)$ can be obtained using the magnetization and its second moment. Finite-size scaling shows that

$$U(t) = \frac{M^{(2)}}{(M)^2} - 1 \sim t^{c_U} \qquad c_U = \frac{d}{z}. \tag{15}$$

Thus, the short-time behaviour of the dynamic relaxation starting from a completely ordered state is also sufficient to determine all the critical exponents $\beta$, $\nu$ and $z$ as well as the critical temperature. In practical simulations, these measurements of the critical exponents and critical temperature are usually better in quality than those from a relaxation process starting from a disordered state.

## 3. Numerical results

We have performed simulations on three-dimensional lattices of linear sizes $L = 32$, 64 and 128 (in a particular case $L = 256$), starting either from an ordered state or from a high-temperature state with zero or small initial magnetization. In the latter cases the inital magnetization has been prepared by flipping in an ordered state a definite number of spins at randomly chosen sites in order to get the desired small value of $m_0$. Starting from the initial state, the system has been updated by a heat bath Monte Carlo algorithm. A unit in time is defined as a complete update of all the spins in the lattice. Simulations have been performed, depending on the inital magnetization, up to $t = 1000$. The preparation of the inital magnetization and the update up to the maximal time has been repeated 1000 or 5000 times, depending on the lattice size (much less for $L = 256$), and the magnetization, the second moment of the magnetization (3) or the autocorrelation (9) has been measured. In general, several runs of this kind have been performed to estimate the statistical error. The simulations used the value $K_c = 0.221\,66$ for the critical point, taken from [10]. Simulations have also been carried out in the neighbourhood of $K_c$ to extract the critical point and the critical exponent $\nu$.

### 3.1. Evolution from a disordered state

*Magnetization.* At the beginning of the time evolution, for sufficiently small $t^{x_0/z}m_0$, the magnetization undergoes a power-law initial increase. For $m_0$ and $t$ not too small, the power-law behaviour will be modified. This may be called the 'finite $m_0$ effect'. The possibility of a finite-size effect also has to be evaluated. Furthermore, scaling form (2) is strictly valid only in the limit $m_0 = 0$. However, practical measurements can only be carried out for finite $m_0$ and the measured exponent $\theta$ may show a weak dependence on $m_0$. The data must thus be extrapolated for $m_0 = 0$.

We have measured the magnetization $M(t)$ for $m_0 = 0.02$, 0.04 and 0.06 for the largest lattice, $L = 128$. For $m_0 = 0.02$ we have performed four runs, in the other cases three runs up to $t = 300$. Figure 1 shows on a log–log scale a pronounced power-law behaviour starting at the onset of the time evolution. A finite $m_0$ effect is observed at the larger times.

In order to determine more clearly the region where the power law is strictly fulfilled, we divided the timescale into non-overlapping intervals $\Delta_q(t) = [t, qt]$, with $q < 2$, and measured the exponent $\theta(t)$ separately in each interval. Since the intervals contain more points at later times where the fluctuations are larger, the errors in each interval are comparable. Already from the second bin the slope shows a stable behaviour. For $m_0 = 0.02$ slope is quite stable up to $t = 100$. Therefore $\theta$ was calculated from a least-squares fit in the time interval [2, 100].

Similarly, we chose the interval [2, 50] for $m_0 = 0.04$. For $m_0 = 0.06$ the restrictive interval [2, 15] was used. Table 1 presents the results. From these results, an extrapolation to
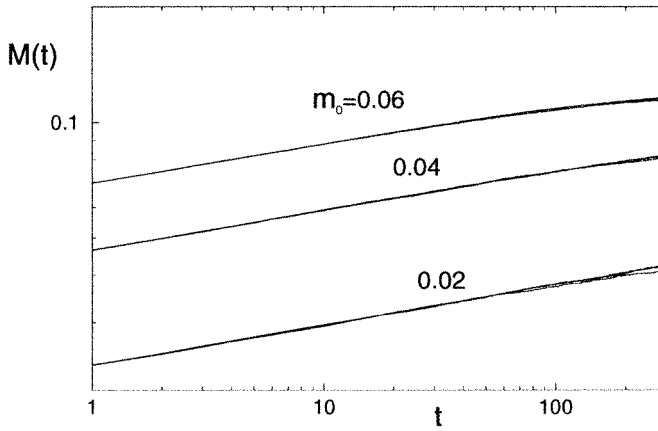
**Figure 1.** Time evolution of the magnetization $M(t)$ for three values of the initial magnetization $m_0$ for $L = 128$.

**Table 1.** The exponent $\theta$ measured for $L = 128$ for different values of the initial magnetization $m_0$. The value $\theta(m_0 = 0)$ is the result of an extrapolation (see text).

| $m_0$ | 0 | 0.02 | 0.04 | 0.06 |
|---|---|---|---|---|
| $\theta$ | 0.108(2) | 0.1059(20) | 0.1035(4) | 0.1014(5) |

$m_0 = 0$ yields $\theta = 0.108(2)$. Careful analysis of the data for $L = 64$ shows that the finite-size effect in $L = 128$ is already negligible.

*Autocorrelation.* Measurements of the autocorrelation function suffer from large fluctuations in the region of large $t$, since it decays by nearly three orders of magnitude between $t = 0$ and $t = 100$. Figure 2($a$) shows results for four runs for $L = 128$ on a log–log scale. For the lattice size $L = 64$ three runs were performed.

As described above, we have divided the timescale into non-overlapping intervals $\Delta_{1.5}(t)$ and calculated $c_a(t)$ in each interval. This is exemplified for $L = 128$ in figure 2($b$). On this plot $c_a(t)$ is rather constant after the first few bins, while large fluctuations start at $t > 70$. Thus, the interval $t = [10, 70]$ is used for $L = 128$ and 64 in order to obtain $c_a$. The results are given in table 2. With no apparent dependence on lattice size, the two results were simply averaged to estimate $c_a$ for $L = \infty$ (second column).

*Second moment of the magnetization.* The second moment of the magnetization has been simulated for $L = 128$ in three runs up to $t = 512$, and for $L = 64$ in three runs each up to $t = 100$. Figure 3 shows $M^{(2)}(t)$ for $L = 128$ on a log–log scale.

This curve as well as the slopes in bins show slightly larger fluctuations at higher $t$, but no departure from a power law. Therefore, the full intervals $t = [2, 512]$ for $L = 128$ and $t = [2, 100]$ for $L = 64$ were used to compute the values of $c_2$ reported in table 2. For $L = \infty$, the estimate $c_2 = 0.970(11)$ provided is obtained by averaging the results for $L = 64$ and $L = 128$, since no dependence on the lattice size can be seen.
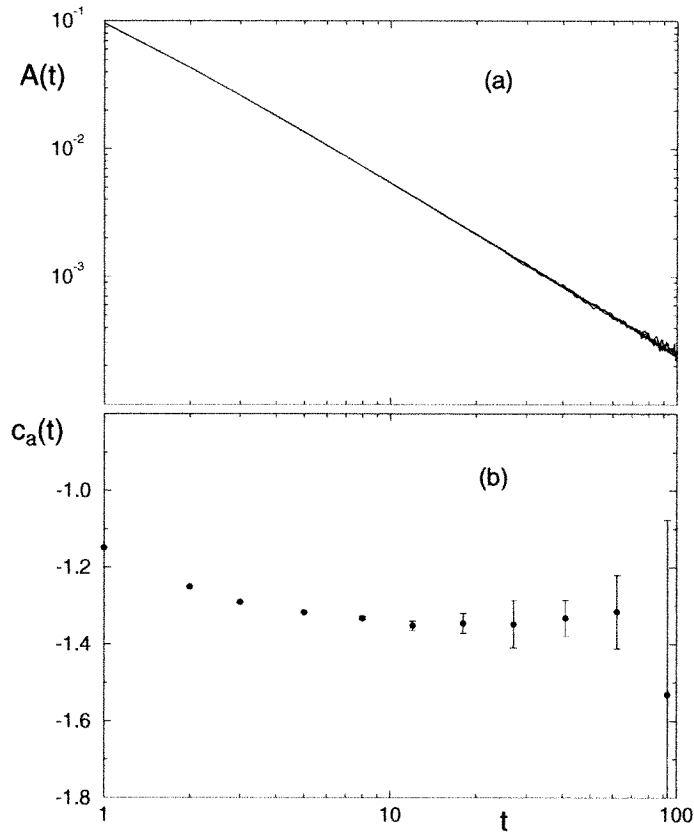
**Figure 2.** (*a*) Autocorrelation $A(t)$ and (*b*) the slope $c_a(t)$ of the autocorrelation function for $L = 128$, in the intervals $\Delta_{1.5}(t) = [t, 1.5t]$.

**Table 2.** Exponents $c_a$ of the autocorrelation function and $c_2$ of the second moment of the magnetization for different lattice sizes obtained from a disordered initial state for $m_0 = 0$ (upper part). Exponents $c_1$ of the power-law decrease of the magnetization and $c_U$ for the cumulant, as well as inverse temperature $K_c$ and exponent $c_{\ell 1}$ for the logarithmic derivative of the magnetization measured from an ordered initial state (lower part). For $c_1$, the additional result $c_1 = 0.2534(4)$ obtained from two runs with $L = 256$ has been included (see text).

|            | $L = \infty$ | $L = 128$  | $L = 64$  |
|------------|-------------|------------|-----------|
| $c_a$      | 1.362(19)   | 1.358(19)  | 1.366(20) |
| $c_2$      | 0.970(11)   | 0.966(16)  | 0.975(3)  |
| $c_1$      | 0.2533(5)   | 0.2539(1)  | 0.2527(8) |
| $c_U$      | 1.462(12)   | 1.453(17)  | 1.471(4)  |
| $K_c$      | 0.221 70(4) | 0.221 70(4)| —         |
| $c_{\ell 1}$ | 0.774(1)  | 0.774(1)   | —         |

## 3.2. Evolution from an ordered state

For the determination of the critical exponents and critical temperature, the dynamic relaxation process starting from an ordered state has been proven advantageous over that from a high-temperature initial state. Indeed, the magnetization only decreases slowly in time from $m_0 = 1$. Furthermore, the magnitude of the magnetization in the short-time regime is large, therefore
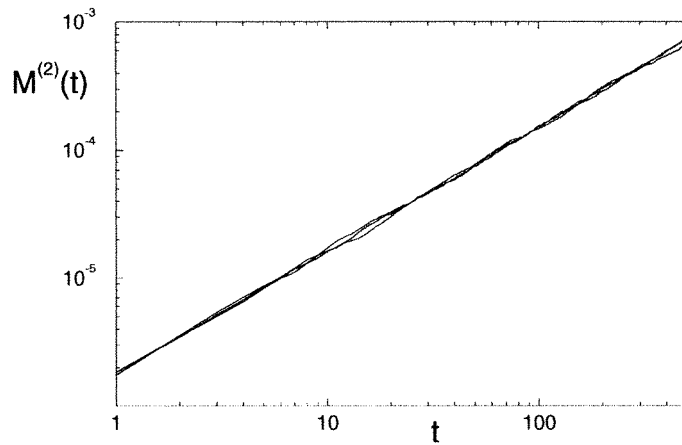
**Figure 3.** Time evolution of the second moment of the magnetization, $M^{(2)}(t)$, for $L = 128$.
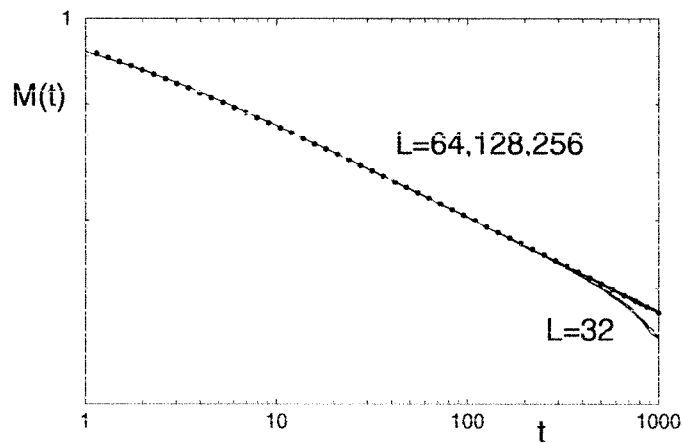


**Figure 4.** Time evolution of the magnetization $M(t)$ for $m_0 = 1$ for $L = 256, 128, 64$ and $32$. The points are obtained from the best fit to (16).

statistical fluctuations are less prominent. We have measured the magnetization $M(t)$ and the second moment $M^{(2)}(t)$ for lattice sizes 32, 64 and 128, and, with less statistics, for $L = 256$. Measurements have been performed up to $t = 512$ for $L = 128$, and up to $t = 1000$ for the magnetization only. For the large lattice size $L = 256$ an average over only 20 samples has been performed whereas for $L = 128$ and 64, over 1000 samples were taken for each run, and two to four runs performed in order to estimate the statistical error. For $L = 32$, 5000 samples were collected.

*Magnetization.* Figure 4 shows the evolution of the magnetization for all four lattice sizes on a log–log scale. It is interesting that for $L = 256$ down to $L = 64$ the measurements completely overlap up to $t = 1000$. From equation (13), the slope of the curves provides a measure of $\beta/\nu z$. However, careful analysis reveals that the slope decreases weakly with increasing time. This suggests that a correction to scaling should be considered in order to obtain accurate results. In comparison to the two-dimensional Ising model, the correction to
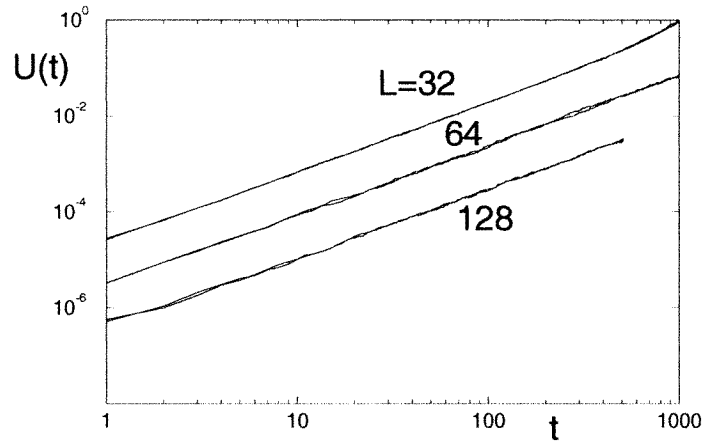
**Figure 5.** Time evolution of the Binder cumulant $U(t)$ for $m_0 = 1$ and lattice sizes $L = 128, 64$ and 32.

scaling seems somewhat larger in three dimensions [2]. We have found that the best correction to scaling is given by the *ansatz*

$$M(t) = at^{-c_1}e^{-\gamma t^{-\delta}}. \tag{16}$$

Least-squares fits were performed in the interval $t = [1, 1000]$ for $L = 64, 128$ and 256. The resulting fit parameters, averaged over the three lattice sizes and over the two runs for each lattice size, are $\ln(a) = 0.0033(10)$, $c_1 = 0.2533(7)$, $\gamma = 0.1874(19)$, and $\delta = 0.479(39)$. Table 2 reports the values for $c_1$. Calculated values for $M(t)$ using (16) are also provided on figure 4 (points) and show good agreement. Without the correction to scaling, the measured exponent $c_1$ would be 1–2% smaller.

*Binder cumulant.*    The second moment of the magnetization has been measured up to $t = 512$ for $L = 128$, and up to $t = 1000$ for $L = 64$ and 32. A plot of the Binder cumulant $U(t)$, defined in equation (15), is shown on log–log scale in figure 5. The curves show that for $L = 32$ the power-law behaviour prevails only up to $t \sim 100$, while for the larger lattices it remains up to the maximal time.

An analysis of the slope measured in the intervals $\Delta_{1.5}(t)$ shows that the exponent $c_U(t)$ can be obtained in the interval $t = 30$ up to the maximal time for $L = 64$ and 128. For $L = 32$ there is a plateau only over $t = [10, 100]$. Hence the results for this lattice size are not reported. The slope $c_U$ is calculated in the intervals $t = [30, 1000]$ for $L = 64$ and $t = [30, 512]$ for $L = 128$ and given in table 2. Within errors they are consistent and their average is reported for $L = \infty$ in table 2. The error estimates are only based on statistics over a limited number of runs and exclude possible systematic contributions.

*Critical temperature and $c_{\ell 1}$.*    Figure 6 shows the magnetization $M(t)$ for $m_0 = 1$ for three values for the inverse temperature $K_1 = 0.220\,66$, $K = 0.221\,66$ and $K_2 = 0.222\,66$, on a log–log scale. The critical point $K_c$ can be estimated by searching for the best power-law behaviour with $K$ between $K_1$ and $K_2$. Namely, the best straight-line fit to curves obtained by quadratic interpolation for $K_1 < K < K_2$ is sought. Restricting the interval to $t = [30, 512]$, the result $K_c = 0.221\,70(4)$ is obtained. The quadratic interpolation also provides the logarithmic derivative of the magnetization with respect to
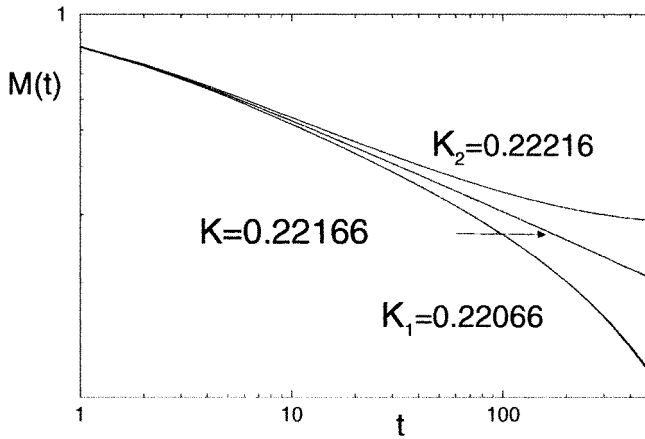
**Figure 6.** Time evolution of the magnetization $M(t)$ for $m_0 = 1$ for three values of the inverse temperature $K_1 = 0.220\,66$, $K = 0.221\,66$ and $K_2 = 0.222\,66$.
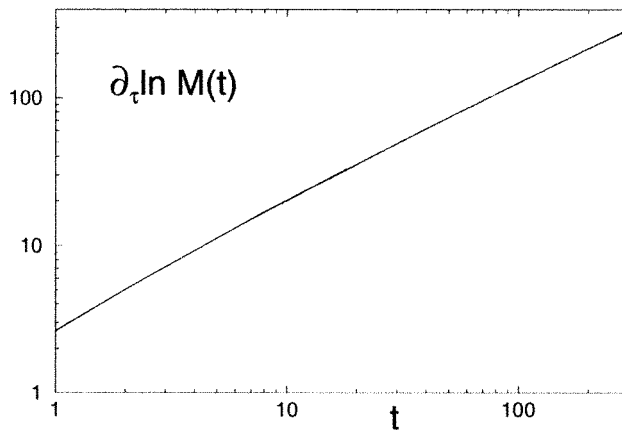


**Figure 7.** Logarithmic derivative of the magnetization with respect to $\tau$, obtained from a quadratic interpolation between the three curves shown in figure 6 taken at $K = 0.221\,66$.

$\tau$ in equation (14). This is shown in figure 7. The slope over the interval $[30, 300]$ provides $c_{\ell 1} = 0.774(1)$. The errors are based on the statistics of comparing only two data sets. A correction to scaling has not been considered. This could result in slightly larger errors.

### 3.3. Critical exponents

We now proceed to determine the critical exponents. Using the relaxation from a high-temperature state, we have measured the exponent $\theta$ directly from the critical initial increase in magnetization (6), and the exponents $c_2$ and $c_a$ from the power-law behaviour of the second moment (8) and the autocorrelation (10). Similarly, from measurements of the power-law behaviour with an *ordered* initial state we have obtained $c_1$, $c_{\ell 1}$ and $c_U$ from the magnetization (13), its logarithmic derivative (14) and the Binder cumulant (15). At this point, it is useful to

**Table 3.** Determination of $z$ from three independent measurements of $d/z$.

|  | $d/z$ | $z$ |
|---|---|---|
| $c_a + \theta$ | 1.470(13) | 2.041(18) |
| $c_U$ | 1.462(12) | 2.052(17) |
| $c_2 + 2c_1$ | 1.4766(8) | 2.032(11) |

**Table 4.** Final results for all critical exponents and the critical point $K_c$ (left). Results from earlier investigations discussed in the text have been collected in the right column.

| $\theta = 0.108(2)$ | 0.104(3) [6] |
|---|---|
| $z = 2.042(6)$ | 2.04(3) [12], 2.032(4) [6] |
|  | 2.04(1) [7], 2.05(2) [3] |
|  | 2.04(2) [4] |
| $\beta/\nu = 0.517(2)$ | 0.518(7) [10], 0.5185(16) [16] |
| $\nu = 0.6327(20)$ | 0.6289(8) [10], 0.6250(25) [11] |
|  | 0.6301(8) [16] |
| $\beta = 0.3273(17)$ | 0.3258(44) [10], 0.3267(10) [16] |
|  | 0.3269(6) [17] |
| $K_c = 0.221\,70(4)$ | 0.221\,6595(26) [10] |
|  | 0.221\,6546(10) [16] |
|  | 0.221\,6544(3) [17] |

recall the scaling relations:

$$c_2 = \frac{d}{z} - 2\frac{\beta}{\nu z} \qquad c_1 = \frac{\beta}{\nu z}$$

$$c_a = \frac{d}{z} - \theta \qquad c_U = \frac{d}{z}$$

$$c_{\ell 1} = \frac{1}{\nu z}.$$

Our measurements of the exponent $c_1$ are very accurate, while actual errors on $K_c$ and $c_{\ell 1}$ could be somewhat larger than those given in table 2. The value obtained for $c_1$ agrees well with previous measurements [3, 4], although the approaches to correct for scaling differ. Our procedure is essentially similar to that used in [11]. The dynamic exponent $z$ can be estimated independently from $c_U$. Since the Binder cumulant (15) is constructed from the magnetization and its second moment, the estimates are usually better than for a Binder cumulant constructed from the second and the fourth moments, typically used in the relaxation from a disordered state or in equilibrium. The exponent $z$ can also be extracted from $c_a + \theta$ and $c_2 + 2c_1$. Table 3 lists the results. These concur within statistical errors. Table 4 reports the average of the three values. With $z$, and from $c_1$ and $c_{\ell 1}$, the exponents $\beta/\nu$ and $\nu$ can be estimated. Results for all critical exponents and the critical point $K_c$ are given in table 4.

Our final result for the exponent $\theta$ given in table 1, $\theta = 0.108(2)$ is consistent with an early estimate using a small lattice [5] but slightly larger than $\theta = 0.104(3)$ obtained from damage spreading [6]. It is not clear whether this difference comes from statistical or systematic errors. From equilibrium dynamics, the dynamic exponent $z = 2.04(3)$ has been extracted [12]. Values of $z = 2.032(4)$ [6] and $z = 2.04(1)$ [7] have been obtained recently from damage spreading and of $z = 2.05(2)$ [3] and $z = 2.04(2)$ [4] from large-scale simulations of critical relaxation, starting from an ordered state. Our value $z = 2.042(6)$ is consistent with all of them. For the ratio $\beta/\nu$ and $\nu$, recent analytic calculations on the

base of a renormalization-group expansion (in equilibrium) yield $\beta = 0.327$, $\beta/\nu = 0.518$ and $\nu = 0.631$ [13–15], while numerical investigations in equilibrium by Ferrenberg and Landau [10] yield $\beta = 0.3258(44)$, $\beta/\nu = 0.518(7)$ and $\nu = 0.6289(8)$. [10] provides a good review of earlier numerical values. Investigations using the cluster algorithm have yielded $\nu = 0.6301(8)$ and $\beta = 0.3267(10)$ [16] and $\beta = 0.3269(6)$ [17]. In [11], the value $\nu = 0.6250(25)$ has been extracted from measuring the interface energy. Our value of $\beta/\nu = 0.517(2)$ is accurate but the value of $\nu$ is slightly larger. Our estimate of $K_c$ is consistent with $K_c = 0.221\,6595(26)$ in [10], $K_c = 0.221\,6546(10)$ [16], or $K_c = 0.221\,6544(3)$ [17]. Similar results have been quoted in [18–20].

## 4. Summary and discussion

In the previous sections we have reported comprehensive Monte Carlo simulations of the short-time critical dynamics for the three-dimensional Ising model. Starting from a high-temperature initial state, the magnetization, its second moment and the autocorrelation have been measured at the critical point. Similarly, we have studied the behaviour of the magnetization, its derivative with respect to the temperature and the Binder cumulant for a completely ordered initial state. Theoretically one expects a power law for all these observables within the short-time regime at the critical point. This is indeed observed in our numerical simulations. All the dynamic exponents and static exponents as well as the critical temperature have been determined. The results are consistent and strongly support a full dynamic scaling in the short-time regime of the dynamic evolution. The values of the dynamic exponent $z$ and the static exponents $\beta/\nu$ and $\nu$ are independent of initial conditions and agree well with those measured in equilibrium. Unlike non-local cluster algorithms, the short-time dynamic approach studies the dynamic properties of the original local dynamics. Our measurements of the static exponents are comparable with large-scale simulations in equilibrium. All this indicates that the dynamic measurements of the critical exponents are promising. This work could possibly be extended to the diluted or the random field Ising models.

*Note added in proof.* Recently, the results $\nu = 0.6298(5)$ [21] and $\beta/\nu = 0.518(1)$ [22] have been reported.

## References

[1] Janssen H K, Schaub B and Schmittmann B 1989 *Z. Phys.* B **73** 539
[2] Zheng B 1998 *Int. J. Mod. Phys.* B **12** 1419
[3] Stauffer D and Knecht R 1996 *Int. J. Mod. Phys.* C **7** 893
[4] Stauffer D 1997 *Physica* A **244** 344
[5] Li Z B, Ritschel U and Zheng B 1994 *J. Phys. A: Math. Gen.* **27** L837
[6] Grassberger P 1995 *Physica* A **214** 547
[7] Gropengiesser U 1995 *Physica* A **215** 308
[8] Janssen H K 1992 From phase transition to chaos *Topics in Modern Statistical Physics* ed G Györgyi *et al* (Singapore: World Scientific)
[9] Schülke L and Zheng B 1996 *Phys. Lett.* A **215** 81
[10] Ferrenberg A M and Landau D P 1991 *Phys. Rev.* B **44** 5081
[11] Ito N 1993 *Physica* A **196** 591

[12] Wansleben S and Landau D P 1991 *Phys. Rev.* B **43** 6006
[13] Guillou J-C L and Zinn-Justin J 1980 *Phys. Rev.* B **21** 3976
[14] Guillou J-C L and Zinn-Justin J 1987 *J. Physique* **48** 19
[15] Antonenko S A and Sokolov A I 1995 *Phys. Rev.* E **51** 1894
[16] Blöte H W J, Luijten E and Heringa J R 1995 *J. Phys. A: Math. Gen.* **28** 6289
[17] Talapov A L and Blöte H W J 1996 *J. Phys. A: Math. Gen.* **29** 5727
[18] Baille C F, Gupta R, Hawick K A and Pawley G S 1992 *Phys. Rev.* B **45** 10 438
[19] Ito N and Suzuki M 1991 J. Phys. Soc. Japan **60** 1978
[20] Ito N 1991 Computer Aided Statistical Physics *AIP Conf. Proc. (New York, 1990)* vol 248 ed C-K Hu (Taipei) p 136
[21] Hasenbusch M, Pinn K and Vinti S 1998 Critical exponents of the 3D Ising universality class from finite size scaling with standard and improved actions *Preprint* hep-lat/9806012
[22] Choi Y S, Machta J, Tamayo P and Chayes L X 1998 Parallel invaded cluster algorithm for the Ising model *Preprint* cond-mat/9806127